1-1-2014

Characterisation of flicker emission and propagation in distribution networks with bi-directional power flows

D Perera
University of Wollongong, bmdp065@uowmail.edu.au

L Meegahapola
University of Wollongong, lasantha.meegahapola@rmit.edu.au

S Perera
University of Wollongong, sarath@uow.edu.au

P Ciufo
University of Wollongong, ciufo@uow.edu.au

Characterisation of flicker emission and propagation in distribution networks with bi-directional power flows

Abstract

With the increasing penetration levels of intermittent and fluctuating energy sources such as wind generating systems in the electricity grid, resulting voltage fluctuations and flicker can be expected to become an important power quality considerations. Due to significant bidirectional power flows resulting from large renewable power generation systems connected to downstream, voltage fluctuations may propagate from downstream to upstream. The work presented in this paper investigates and characterises flicker emission and propagation resulting from fluctuating generating sources connected to a distribution network. Mathematical models are developed for flicker emission under different generator control strategies and flicker propagation to upstream network. These emission and propagation characteristics are investigated and verified using a test network comprised of a wind farm. The study has revealed that flicker emission characteristics are influenced in a detrimental manner by the reactive power control strategy of the generator and the flicker attenuation characteristics are influenced by the various load types connected to the distribution feeder.

Keywords

propagation, distribution, networks, bi, directional, power, characterisation, flows, flicker, emission

Disciplines

Engineering | Science and Technology Studies

Publication Details

D. Perera, L. Meegahapola, S. Perera & P. Ciufo, "Characterisation of flicker emission and propagation in distribution networks with bi-directional power flows," Renewable Energy, vol. 63, pp. 172-180, 2014.

Characterisation of Flicker Emission and Propagation in Distribution Networks with Bi-directional Power Flows

D. Perera, L. Meegahapola, S. Perera, P. Ciufo*

Australian Power Quality and Reliability Centre, School of Electrical, Computer, and Telecommunications Engineering, University of Wollongong, Wollongong, New South Wales 2522, Australia

Abstract

With the increasing penetration levels of intermittent and fluctuating energy sources such as wind generating systems in the electricity grid, resulting voltage fluctuations and flicker can be expected to become an important power quality considerations. Due to significant bidirectional power flows resulting from large renewable power generation systems connected to downstream, voltage fluctuations may propagate from downstream to upstream. The work presented in this paper investigates and characterises flicker emission and propagation resulting from fluctuating generating sources connected to a distribution network. Mathematical models are developed for flicker emission under different generator control strategies and flicker propagation to upstream network. These emission and propagation characteristics are investigated and verified using a test network comprised of a wind farm. The study has revealed that flicker emission characteristics are influenced in a detrimental manner by the reactive power control strategy of the generator and the flicker attenuation characteristics are influenced by the various load

*Corresponding author. Tel +61242213406 Fax. +61242213236

Email addresses: bmdp065@uowmail.edu.au (D. Perera), lasantha@uowmail.edu.au (L. Meegahapola), sarath@uow.edu.au (S. Perera), ciufo@uow.edu.au (P. Ciufo)

[1]NOTICE: this is the authors' version of a work that was accepted for publication in Renewable Energy. Changes resulting from the publishing process, such as peer review, editing, corrections, structural formatting, and other quality control mechanisms may not be reflected in this document. Changes may have been made to this work since it was submitted for publication. A definitive version was subsequently published in Renewable Energy, [vol. 63, pages 172-180 (Mar. 2014)] DOI:10.1016/j.renene.2013.09.007

types connected to the distribution feeder.

Keywords: Doubly-fed induction generator (DFIG), flicker, power factor control, voltage control, voltage fluctuations, wind generation.

---

1. Introduction

Existing studies on flicker emission and propagation due to renewable energy generators (REGs) such as DFIG wind turbines are largely based on their unity power factor operation [1–9]. Limited research outcomes exist [5] investigating the dependence of flicker emission on the intermittency of renewable energy resources and network parameters such as grid impedance angle, short-circuit capacity of the grid. Modern REGs such as doubly-fed induction generators (DFIGs) have proven reactive power capabilities [10] which enable them to operate in various control modes such as power factor control and voltage control operation. In future, REGs will be required to operate under different control strategies in order to provide ancillary services such as reactive power support and system voltage control to the power network [11]. Only limited studies exist on the impact on flicker emission when REGs are operating under such control strategies [12].

The existing literature provides a comprehensive understanding on flicker propagation and attenuation [13–16] in radial networks, essentially related to fluctuating loads where the active and reactive power flows are unidirectional, i.e upstream to downstream. In distribution networks with embedded generation, active and reactive power flow could become bi-directional. Moreover, the connected loads in such networks can also influence flicker propagation and attenuation. Although flicker propagation and attenuation associated with induction motors has been well researched [17, 18], the flicker propagation and attenuation due to other load types such as constant power and constant current loads have not been adequately addressed. A comprehensive understanding of flicker propagation and attenuation features of such loads can help in the effective planning and management of distribution networks which may have high levels of integrated REGs.

The main objective of the work presented in this paper is to provide a comprehensive analysis on the impact of reactive power control strategies of REGs when they provide ancillary services to the network and to study the influence of different distribution system loads on flicker emission and propagation in radial distribution networks where there is bi-directional power

flow. Mathematical models are developed and are verified using a simulation model of a wind farm in DIgSILENT Power Factory software [10], [19–21].

The paper is structured as follows: theoretical analysis on the flicker emission and propagation under power factor control and voltage control operation of a REG in general is given in Section 2. Section 3 presents a case study distribution system verifying the conclusions of Section 2. The response of the distribution system loads to voltage fluctuations; hence, flicker and its relationship with flicker emission of the REG is discussed in Section 4 through appropriate mathematical models. The simulation model of Section 3 is further extended in Section 5 to characterise the influence of distribution system loads on flicker emission and propagation. Conclusions are given in Section 6.

2. Dependency of Flicker Emission and Propagation on REG Control Strategies

In order to investigate the impact of a reactive power control strategy on flicker emission from a REG, a radial network model shown in Fig. 1 is considered.

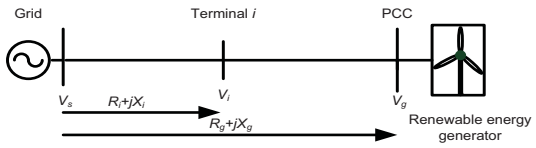

Figure 1: Renewable energy generator connected to a radial network

V_s, V_g,V_i, denote the grid voltage, voltage at the PCC of the REG and voltage at an intermediate terminal i respectively. Due to the intermittent nature of the renewable energy generator, its active and reactive power output is considered to fluctuate, which leads to fluctuations in the PCC voltage. The phasor representation of the voltage fluctuation at the PCC is illustrated in Fig. 2. The convention used in the context of the paper is as follows: when the REG is supplying both active and reactive power to the network at the PCC the REG is said to operate at a leading power factor (as shown in Fig. 2). When the REG is supplying active power while absorbing reactive power, REG is said to operate at a lagging power factor.

$V_{g,\mathrm{pre}}$, $V_{g,\mathrm{post}}$ are the voltages at the PCC of the generator pre and post power fluctuation, ΔI_g is the fluctuation in generator current, R_g and X_g are

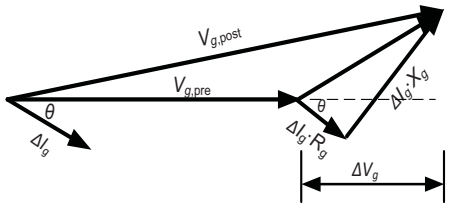

Figure 2: Vector diagram of the voltage fluctuation due to generator output power fluctuation [22]

the Thévenin resistance and reactance at the PCC of the REG and θ is the angle of generator real (ΔP) and reactive output power fluctuation (ΔQ), (i.e. $\arctan(\frac{\Delta Q}{\Delta P})$). The voltage fluctuation ΔV_g at the PCC of the REG is approximately given by Eq. (1),

$$\Delta V_g \approx \Delta I_g \cdot (R_g \cdot \cos\theta + X_g \cdot \sin\theta) \tag{1}$$

The relative voltage fluctuation at the PCC of the REG can be approximately expressed in terms of ΔP and ΔQ as Eq. (2),

$$\left|\frac{\Delta V_g}{V_g}\right| \approx \left|\frac{\Delta P \cdot R_g + \Delta Q \cdot X_g}{V_g^2}\right| \tag{2}$$

Similarly, considering the intermediate terminal i in the radial distribution system given in Fig. 1, its relative voltage fluctuation due to fluctuation of active and reactive power output of the REG can be given by Eq. (3),

$$\left|\frac{\Delta V_i}{V_i}\right| \approx \left|\frac{\Delta P \cdot R_i + \Delta Q \cdot X_i}{V_i \cdot V_g}\right| \tag{3}$$

where the Thévenin resistance and reactance at the i^{th} terminal of the network are R_i and X_i respectively.

Hence, the relative voltage fluctuation transfer coefficient between the PCC and intermediate terminal i, $T_{\Delta V_{g,i}}$ can be written as Eq. (4),

$$T_{\Delta V_{g,i}} \approx \frac{|\Delta V_i/V_i|}{|\Delta V_g/V_g|} = \left|\frac{\Delta P \cdot R_i + \Delta Q \cdot X_i}{\Delta P \cdot R_g + \Delta Q \cdot X_g} \cdot \frac{V_g}{V_i}\right| \tag{4}$$

Assuming that the range of frequency of voltage fluctuations is very limited, the relative voltage fluctuations and relative voltage fluctuation transfer coefficient can be correlated to flicker and flicker transfer coefficient. Therefore,

the flicker transfer coefficient from the PCC of REG to terminal i of the network can be approximated by Eq. (4).

According to Eq. (2) and Eq. (4), flicker emission from the REG and flicker propagation to upstream of a radial network are dependent on active and reactive power fluctuations and network impedance. The active power fluctuations depend on the renewable energy source while the reactive power fluctuations depend on the control strategy of the REG.

The impact of (a) power factor control (b) voltage control and (c) reactive power dispatch of the REG on flicker emission and propagation are discussed in the following sections.

2.1. Power Factor Control Mode

Power factor control can be implemented in REGs in which the operating power factor of the REG is maintained at a fixed value irrespective of output power fluctuations. Assuming an operating power factor of $cos\phi$ for the REG, where ϕ is the power factor angle, the fluctuation in real and reactive power will be such that Eq. (5),

$$\Delta Q = \Delta P \cdot \tan\phi \tag{5}$$

By substituting Eq. (5) in Eq. (2), the relative voltage fluctuation at the PCC of the REG can be obtained as Eq. (6),

$$\left|\frac{\Delta V_g}{V_g}\right| \approx \left|\frac{\Delta P \cdot (R_g + \tan\phi \cdot X_g)}{V_g^2}\right| \tag{6}$$

Note that the angle of generator output active and reactive power fluctuation θ in Fig. 2 is equal to the operating power factor angle ϕ of the REG in power factor operation mode, as the pre and post power fluctuation power factors of the REG are identical. Equation (6) can be further simplified to Eq. (7),

$$\left|\frac{\Delta V_g}{V_g}\right| \approx \frac{\Delta S}{S_{sc,g}} \cdot \cos(\varphi - \phi) \tag{7}$$

where ΔS, $S_{sc,g}$, φ are VA output fluctuation of the REG, short-circuit capacity at the PCC of the REG and the grid impedance angle ($\arctan(\frac{X_g}{R_g})$) as seen by the REG respectively. According to Eq. (7), flicker emission by a REG is dependent on its operating power factor. It can be noted that if the operating power factor is maintained such that $\phi = -\Pi/2 + \varphi$, the relative

voltage fluctuation at the PCC in Eq. (7) would be zero. This ideal observation results from the approximation made in the derivation of Eq. (1) but in practice some flicker will exist.

The corresponding relative voltage fluctuation at the intermediate terminal i is given by Eq. (8),

$$\left|\frac{\Delta V_i}{V_i}\right| \approx \left|\frac{\Delta P \cdot (R_i + \tan\phi \cdot X_i)}{V_i \cdot V_g}\right| \tag{8}$$

The flicker transfer coefficient between the PCC of the REG and intermediate terminal i can be written as Eq. (9),

$$T_{\Delta V_{g,i}} \approx \left|\frac{R_i + \tan(\phi) \cdot X_i}{R_g + \tan(\phi) \cdot X_g} \cdot \frac{V_g}{V_i}\right| \tag{9}$$

Assuming $V_i \approx V_g$, Eq. 9 can be approximated as Eq. 10,

$$T_{\Delta V_{g,i}} \approx \left|\frac{R_i + \tan(\phi) \cdot X_i}{R_g + \tan(\phi) \cdot X_g}\right| \tag{10}$$

According Eq. (10), flicker propagation from the PCC of the REG to upstream of the network is dependent on the operating power factor of the REG. It has to be noted that Eq. (10) leads to greater error when applied for lagging power factor cases compared to leading power factor cases because of the cancellation which takes place in both the numerator and denominator of the RHS of Eq. (10).

2.2. Voltage Control Mode

A voltage control strategy associated with reactive power can also be employed in REGs for voltage stability improvement and network voltage profile management. In the voltage control mode, the relative voltage fluctuations at the PCC should be of zero magnitude. However, due to fast variations of the power levels associated with REG, the voltage controller of the REG may not be capable of achieving zero relative voltage fluctuations; hence, leading to some flicker level at the PCC.

To achieve zero voltage fluctuation at the PCC of the REG the required theoretical level of ΔQ can be determined as Eq. (11),

$$\left|\frac{\Delta V_g}{V_g}\right| \approx \left|\frac{\Delta P \cdot R_g + \Delta Q \cdot X_g}{V_g^2}\right| \approx 0 \Rightarrow \Delta Q \approx \frac{-R_g}{X_g} \cdot \Delta P \tag{11}$$

Substituting the end result for ΔQ of Eq. (11) in Eq. (3), the relative voltage fluctuation at the intermediate terminal i of the network can be written as Eq. (12),

$$\left|\frac{\Delta V_i}{V_g}\right| \approx \left|\Delta P \cdot \frac{R_i - \frac{R_g}{X_g} \cdot X_i}{V_i \cdot V_g}\right| \tag{12}$$

According to Eq. (12), there will be no voltage fluctuations at the PCC when $R_i = R_g$ and $X_i = X_g$. As the location of interest moves away from the PCC, the term $|R_i - \frac{R_g}{X_g} \cdot X_i|$ increases up to a certain point along the feeder (e.g. transformer secondary) leading to increased flicker levels. Beyond that point (e.g. on the HV side of the transformer), the term $|R_i - \frac{R_g}{X_g} \cdot X_i|$ reduces to a lower value, due to sudden reduction of X_i (e.g. transformer reactance). Hence, flicker levels would decrease to a relatively a lower value.

2.3. Reactive Power Dispatch Mode

In the reactive power dispatch mode, the REG will dispatch a fixed amount of reactive power, irrespective of active power fluctuations. Hence, the voltage fluctuations and flicker will be dependent only on active power fluctuations. This is similar to unity power factor operation considered in Section 2.1 because there is no reactive power fluctuations. Therefore, no further analysis is required.

3. Impact of Wind Farm Control Strategies on Flicker Emission and Propagation: Case Study

Flicker emission from a wind farm and associated propagation of flicker to the upstream network was studied using the network shown in Fig. 3 employing different control strategies under varying wind conditions [10]. A 19.5 MW wind farm consisting of 13, 1.5 MW DFIG generators connected to a 33 kV 15 km long distribution line was modelled in DIgSILENT Power Factory using an aggregated wind farm model [10], [19–21]. The network and DFIG machine parameters are given in Appendix Appendix B. A wind profile with a mean wind speed of 7.5 m/s [2]and turbulence intensity of 0.1 was used in the simulations. The short-term flicker severity levels at the PCC

[2]For a typical wind turbine, the cut in, cut out and rated wind speed is 3.5 m/s, 25 m/s and 12 m/s respectively [23]. The wind speed of 7.5 m/s was selected for the simulation

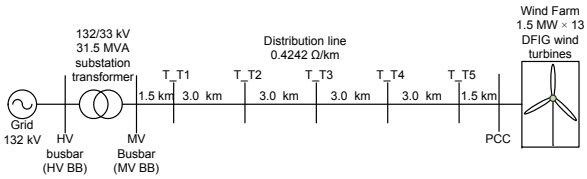

Figure 3: Single line diagram of the MV network

of the wind farm and at the intermediate terminals in the network T_T1 to T_T5, MV busbar and HV busbar were measured using a flickermeter [24].

3.1. Power Factor Control Mode

Fig 4 (a)-(b)[3] illustrate the flicker emission from the wind farm, when the wind farm operating over a range of power factors considering the future requirement where wind farms are required to provide reactive power support to the network due to displaced synchronous generators. Flicker emission at the unity power factor in which most of the existing wind farms are operated, is significantly less compared to leading power factor operation as shown from Fig 4 (a)-(b). Furthermore, according to Fig. 4 (a) , dependency of flicker emission from the wind farm on the operating power factor and distribution line X/R ratio as suggested by Eq. (7) is evident. For a distribution line having a unity X/R ratio, the short-term flicker severity reaches 0.36 when the wind farm is operating at 0.90 leading power factor. For the same line the short-term flicker severity is 0.19 if operated at unity power factor, which further reduces to 0.14 at an operating power of 0.95 lagging. This characteristic can be explained referring to Eq. (6), for a leading power factor, the term $(\Delta P \cdot R_g)$ associated with real power fluctuations and the term $(\Delta P \cdot \tan(\phi) \cdot X_g)$ associated with reactive power fluctuations

considering the reactive power capabilities of the grid side and rotor side converters of the DFIG [10]. The selected wind speed ensures that the reactive power capabilities of the DFIG are not exceeded under high wind gust situations, therefore, the wind farm can be operated under investigated reactive power control strategies.

[3]Fig. 4-(a) illustrates the flicker emission from the wind farm when the distribution line impedance was maintained constant at 0.4242 Ω/km, while the X/R ratio of the distribution line varies. Fig. 4-(b) illustrates , the flicker emission from the wind farm when the distribution line impedance was maintained constant, at $0.3 + \mathrm{j}0.3$ Ω/km, while the short-circuit capacity of the HV distribution network varies.

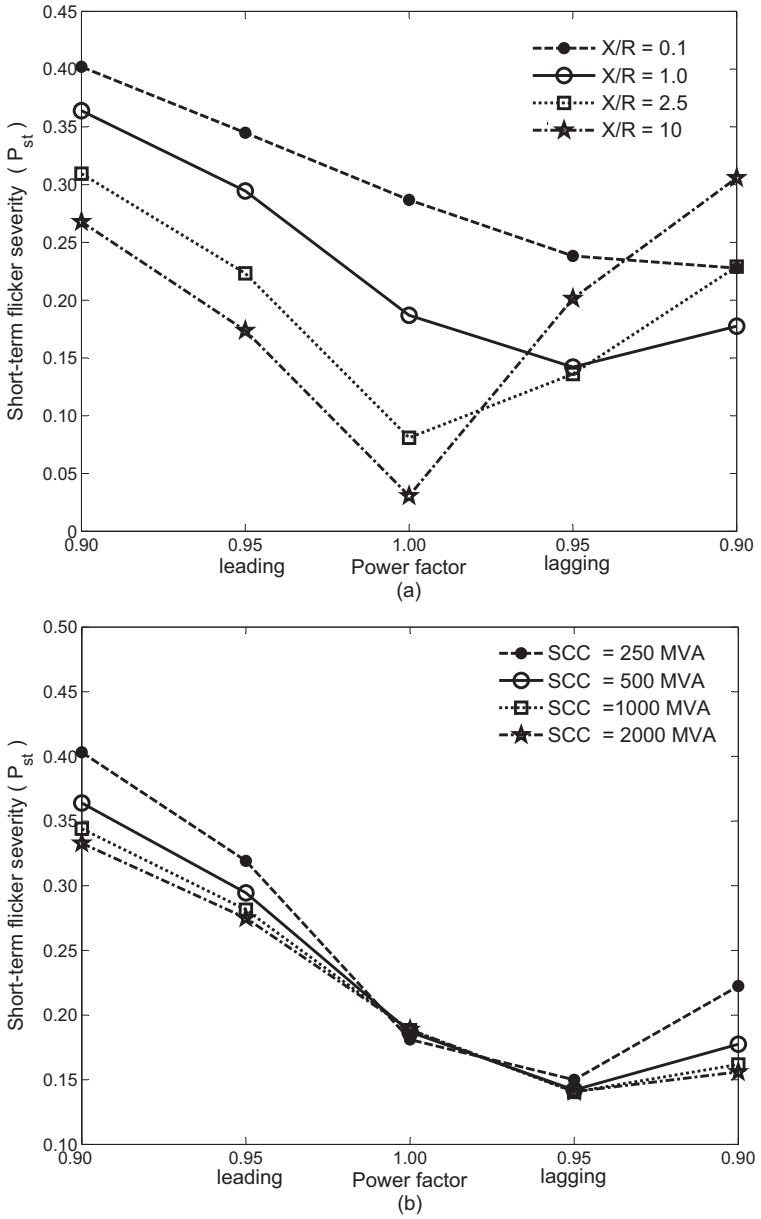

Figure 4: Short-term flicker severity at the PCC of the wind farm for different power factors when, (a) distribution line X/R ratio varies; (b) short-circuit capacity of the HV grid varies;

reinforce each other. On the contrary, for lagging power factors, the influence of active power fluctuations on voltage is counteracted by the voltage fluctuations associated with reactive power, thus reducing the resultant relative voltage fluctuations; hence, the flicker emission. According to Eq. (7), the voltage fluctuations caused by the active power fluctuations completely nullifies the voltage fluctuations caused by the reactive power fluctuations when the operating power factor angle ϕ is equal to $-\Pi/2 + \varphi$; hence, the relative voltage fluctuations would be zero thus giving rise to zero flicker. However, this is an ideal outcome that results from the approximation made in deriving Eq. (1). For an operating power factor of 0.90 lagging, the short-term flicker severity has increased to 0.18 from 0.14 which results from the dominance of the voltage fluctuations associated with reactive power fluctuations compared to same corresponding to real power fluctuations (i.e. $\Delta P \cdot \tan(\phi) \cdot X_g > \Delta P \cdot R_g$).

Further observations can be made with respect to other distribution line X/R ratios from which it can be seen that the power factor at which minimum flicker emission occur depends on the X/R ratio of the distribution line. Due to the control gains and time delays associated with the DFIG controls the instantaneous power factor of the wind farm can slightly vary from the fixed value. This aspect is not considered in derivation of Eq. (7). Therefore, the power factor at which minimum flicker occurs will be slightly different from the theoretical value obtained from Eq. (7).

When the wind farm is operating at leading or unity power factors, flicker emission will decrease in relation to lines having higher X/R ratios. In contrast, at lagging power factors the flicker emission can be observed to increase with the distribution line X/R ratio. For instance, the short-term flicker levels are 0.30, 0.23 and 0.18 respectively for distribution lines with X/R ratios of 10, 2.5 and 1.0 when the wind farm is operating at a lagging power factor of 0.90. This characteristic is due to the increased dependency of voltage fluctuations on reactive power fluctuations; hence, line reactance.

As expected, Fig. 4-(b) illustrates that if the wind farm is connected to a weak HV grid (i.e. 132 kV network), the flicker levels at the PCC become marginally higher for a fixed power factor, compared to the case of a strong HV grid, resulting from the relatively higher grid impedance in the former case. Moreover, HV grid impedance is mainly reactive. Therefore, short-term flicker severity levels do not appreciably change at unity power factor (because the voltage fluctuations are independent of line reactance at unity power factor) as the short-circuit capacity of the HV grid increases.

Fig. 5(a) and (b) illustrate the flicker levels at different terminals of the network for various distribution line X/R ratios for a leading power factor of 0.95 and a lagging power factor of 0.95. For operation at the leading power factor, flicker levels decrease as the point of observation moves away from the PCC of the wind farm towards the HV grid irrespective of the distribution line X/R ratio as expected. However, for the operation at lagging power factor, the flicker levels do not diminish as the HV grid is approached. For instance, when the wind farm is operating at the lagging power factor of 0.95 with the distribution line with unity X/R ratio, slightly higher flicker levels can be observed at the MV busbar compared to downstream intermediate terminals. Minimum levels of flicker can be observed at the terminal T_T2. For lagging power factor operation, the voltage fluctuations at the terminal T_T2 due to active power fluctuations ($\Delta P \cdot R_i$) is counteracted by the voltage fluctuations due to reactive power fluctuations ($\Delta P \cdot \tan(\phi) \cdot X_i$) resulting a minimum flicker (according to Eq. (8)). However, at the MV busbar, the dependency of the voltage fluctuations on reactive power fluctuations is greater than that due to active power fluctuations as $R_i < X_i$. Accordingly, the flicker levels at the MV busbar will be greater compared to that at terminal T_T2. In contrast, with higher distribution line X/R ratios, the voltage fluctuations at intermediate points of the network are mainly dependent on reactive power fluctuations and the effective reactances seen at those points. Hence, local minimum locations for flicker levels are observed along the feeder.

Fig. 6 provides a comparison of the flicker transfer coefficients estimated using Eq. (9) with the values obtained through simulations, for the wind farm operating with a distribution line having a unity X/R ratio. The estimated transfer coefficients are marginally larger than those obtained from simulations for unity power factor operation where the flicker transfer coefficient is essentially governed only by the Thévenin resistance associated with the fault level at the locations under consideration. This discrepancy arises as a result of the small amount of reactive power injection/absorption associated with the wind farm even at unity power factor operation (due to reactive power controller of the DFIG not being fast enough to respond to the active power fluctuations) thus affecting the flicker values.

3.2. Voltage Control Mode

Operation of the wind farm whilst maintaining a PCC voltage of 1.05 pu is considered. According to Fig. 7(a), higher flicker levels are observed at

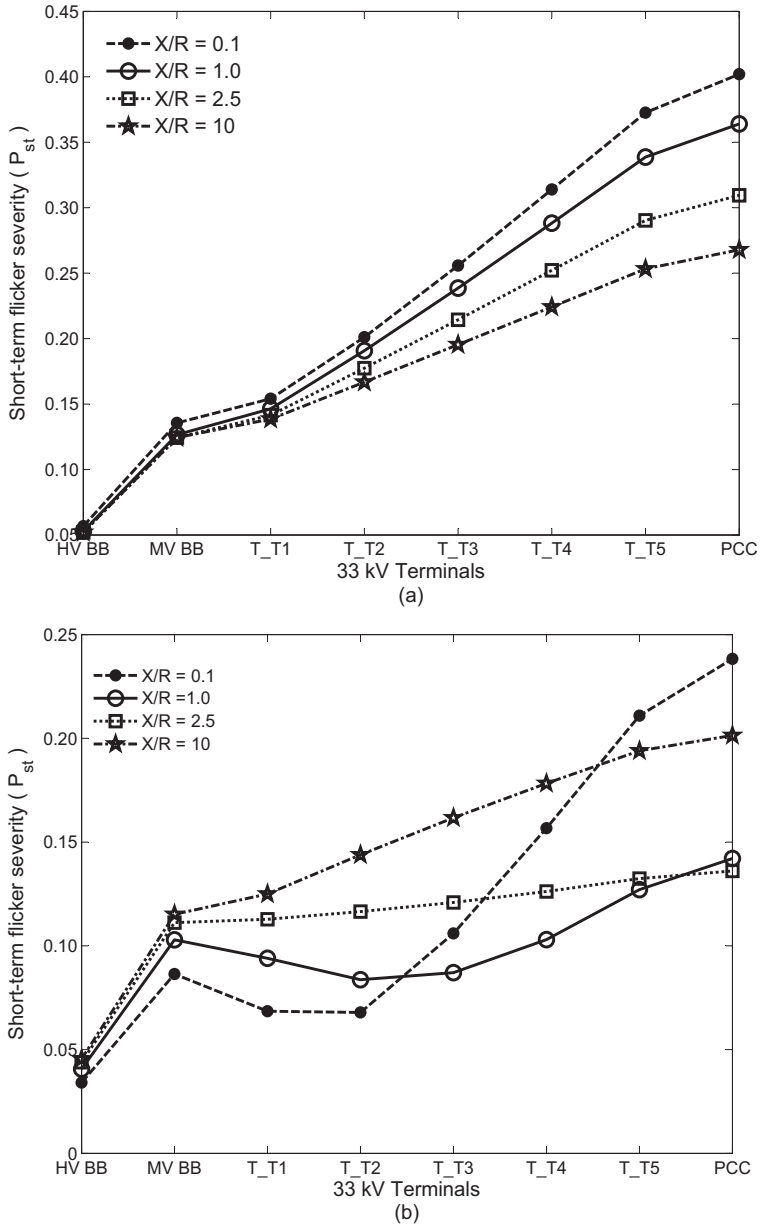

Figure 5: Short-term flicker severity at different terminals of the network when the wind farm operating in (a) leading power factor of 0.95; (b) lagging power factor of 0.95;

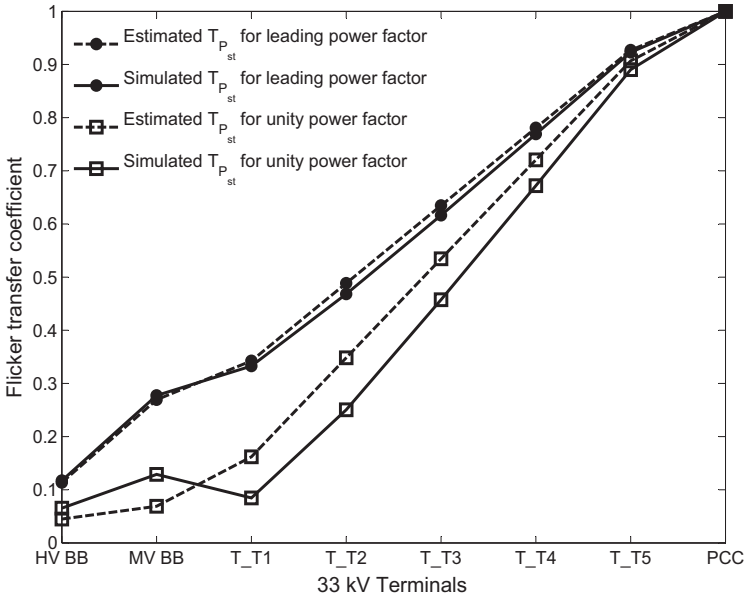

Figure 6: Comparison between the estimated values and simulation results of flicker transfer coefficient

the PCC of the wind farm when it is connected to a distribution line with a low X/R ratio. As an example, for the line with a low X/R ratio of 0.1, the flicker severity at the PCC decreases from 0.08 to 0.04 when the wind farm is connected to a distribution line having an X/R ratio of 2.5.

Fig 7(b) illustrates that the flicker emission from the wind farm (measured at the PCC) has marginally increased for the HV grid with a greater short-circuit capacity. For instance, flicker level increased from 0.02 to 0.04 (although very small), when the short-circuit capacity of the HV grid increases from 250 MVA to 1000 MVA. The reason for this being that the HV grid will influence the reactive power fluctuations required to maintain the PCC voltage at the reference value. For the given case, the reactive power fluctuations associated with the wind farm to maintain the PCC voltage are greater when the short-circuit capacity of the HV grid is 1000 MVA than in comparison to short-circuit capacity of 250 MVA.

In addition, Fig. 7(a) and (b) illustrate that the flicker levels increase and reach a maximum value as the point of observation moves away from the PCC of the wind farm which then decrease. This characteristic behaviour was explained in Section 2-B. As expected, the propagation of flicker to

upstream network significantly reduces when strong HV grids are utilised for the connection of wind farms as illustrated in Fig. 7(b).

4. Dependency of Flicker Propagation on Distribution Loads

4.1. Impact of Distribution Load Types on Flicker Propagation

In radial power systems, the upstream to downstream flicker transfer is dependent on downstream load composition [15]. Consider a radial distribution network as shown in Fig. 8 where a distribution load is connected to a fluctuating source by a network impedance. The voltage fluctuation transfer coefficient between the source and the load, $T_{\Delta \mathrm{V_{S,L}}}$ for the network can be expressed as Eq. (13)[15],

$$T_{\Delta \mathrm{V_{S,L}}} \approx \frac{\left|\frac{\Delta V_L}{V_L}\right|}{\left|\frac{\Delta V_S}{V_S}\right|} = \frac{\left|1+\frac{Z_s}{Z_L}\right|}{\left|1+\frac{Z_s}{Z'_L}\right|} \tag{13}$$

where V_S, V_L are the magnitudes of the steady-state voltages at source and load terminals, ΔV_S, ΔV_L are voltage fluctuations at source and load terminals, Z_L is the steady-state impedance of the load, Z'_L is the dynamic impedance of the load to small voltage fluctuations and Z_S is the impedance of the supply system (i.e. sum of the steady-state impedances of the transformers and the distribution line). Dynamic impedance of a R-L type load (i.e. constant impedance load) is approximately equal to its steady-state impedance, whereas for induction motor loads, dynamic impedance is less than the steady-state impedance [15]. However, based on the load characteristics (i.e. constant power load, constant current load), the dynamic impedance of a load can vary from its steady-state impedance value. In the following sections, the flicker attenuation characteristics of constant power, constant current, constant impedance and ZIP loads are briefly discussed.

4.1.1. Constant power loads

For the situation as shown in Appendix A, the relative voltage fluctuation transfer coefficient takes the form of Eq. (14),

$$T_{\Delta \mathrm{V_{S,L}}} = \frac{\left|\frac{\Delta V_L}{V_L}\right|}{\left|\frac{\Delta V_S}{V_S}\right|} = \left|\frac{1+\frac{P_L \cdot R_S + Q_L \cdot X_S}{V_L^2}}{1-\frac{P_L \cdot R_S + Q_L \cdot X_S}{V_L^2}}\right| \tag{14}$$

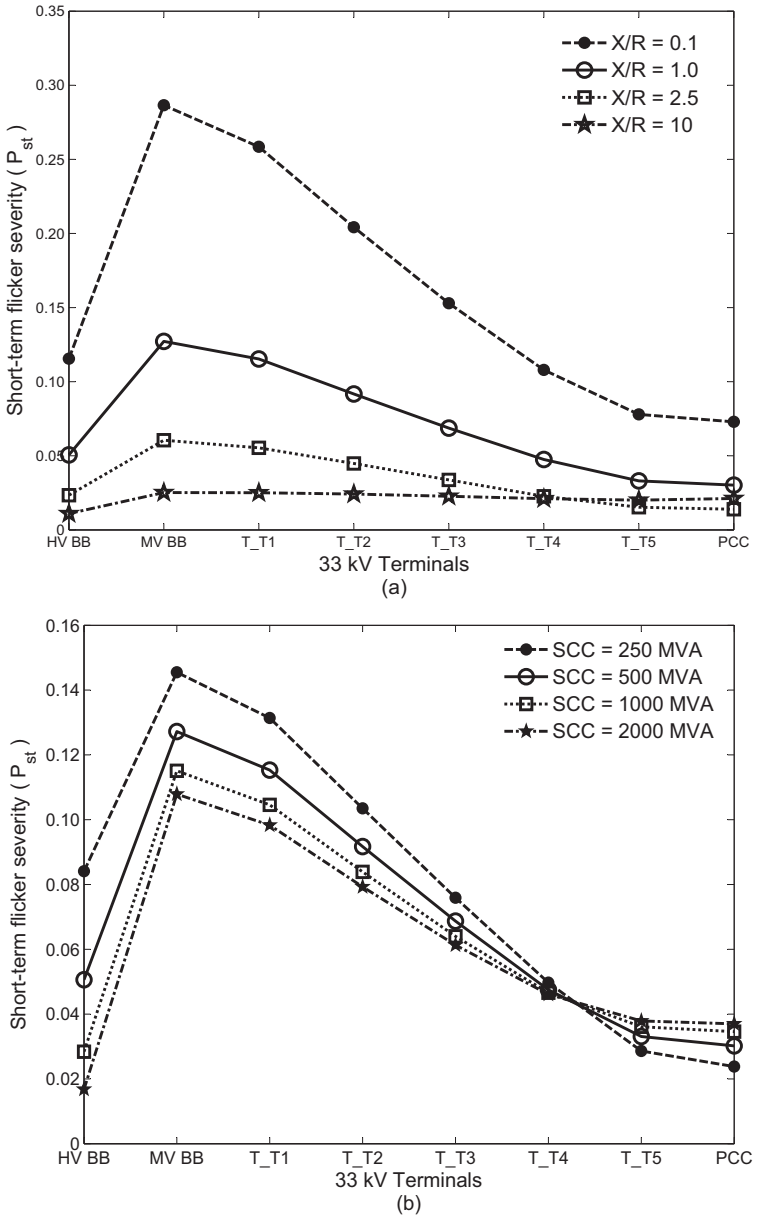

Figure 7: Short-term flicker severity at different terminals of the network when the wind farm operating in voltage control mode when, (a) distribution line X/R ratio varies; (b) short-circuit capacity of the HV grid varies;

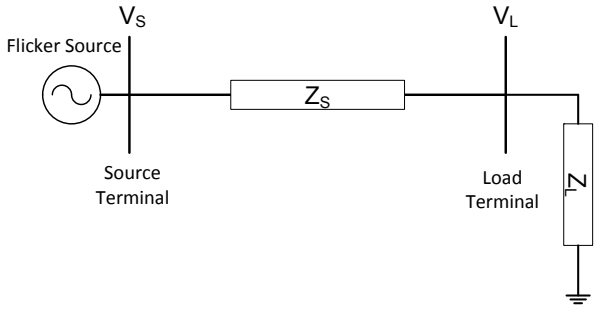

Figure 8: Radial power system

Examination of Eq. (14) indicates that $T_{\Delta V_{S,L}} \geq 1$, for constant power loads with a lagging power factor. Hence, constant power loads will exacerbate the flicker levels at the load terminal when connected to a fluctuating upstream source by a network impedance.

4.1.2. Constant current loads

Constant current loads will maintain the magnitude of the current constant, irrespective of the load terminal voltage. Thus,

$$\Delta V_L = \Delta V_S \tag{15}$$

Hence $T_{\Delta V_{S,L}}$ can be written as Eq. (16),

$$T_{\Delta V_{S,L}} = \left| 1 + \frac{P_L \cdot R_S + Q_L \cdot X_S}{V_L^2} \right| \tag{16}$$

Referring to Eq.(16), $T_{\Delta V_{S,L}} \geq 1$ for constant current loads with lagging power factor; hence, the flicker will exacerbate at the load terminal as in the case of constant power loads.

4.1.3. Constant impedance loads

If a constant impedance load with a capacity of $P_L + jQ_L$ is connected to the load terminal, the fluctuation of load current ΔI_L can be written as Eq. (17),

$$\Delta I_L \approx (P_L - jQ_L)\frac{\Delta V_L}{V_L^2} \tag{17}$$

Hence, $\Delta V_L/\Delta V_S$ can be written as Eq. (18),

$$\left|\frac{\Delta V_L}{\Delta V_S}\right| = \left|\frac{1}{1+\frac{P_L \cdot R_S + Q_L \cdot X_S}{V_L^2}}\right| \tag{18}$$

Therefore, considering Eq. (18) and Eq. (A.9), $T_{\Delta \mathrm{V_{S,L}}}$ can be found to be equal to unity. Therefore, the flicker levels at the load terminal will remain equal to that of the source terminal as expected.

4.1.4. ZIP loads

Assume a mix of parallel connected constant power, constant current and constant impedance loads connected at the load busbar. In this case $T_{\Delta \mathrm{V_{S,L}}}$ can be written as Eq. (19),

$$T_{\Delta \mathrm{V_{S,L}}} = \frac{\left|\frac{\Delta V_L}{V_L}\right|}{\left|\frac{\Delta V_S}{V_S}\right|} = \left|\frac{1+\frac{P_L \cdot R_S + Q_L \cdot X_S}{V_L^2}}{1-\frac{(K_1-K_3)\cdot(P_L \cdot R + Q_L \cdot X)}{V_L^2}}\right| \tag{19}$$

where K_1, K_2 and K_3 are ratios of capacity of constant power, constant current and constant impedance loads to the total capacity of the load respectively and $K_1 + K_2 + K_3 = 1$. Therefore, upstream to downstream flicker propagation will depend on K_1, K_2 and K_3. Furthermore, when $K_1 = K_3$ flicker attenuation characteristics of a ZIP load will be similar to that of a constant current load.

4.1.5. Induction motor loads

The flicker attenuation characteristics of induction motors are well documented in [17], [18] where flicker transfer coefficient is shown to be less than unity for most modulation frequencies in a sinusoidally modulated flicker scenario. However, when the modulation frequency extremely low, the flicker levels at the source terminals can be magnified [18].

4.2. Impact of Distribution Loads on Flicker Emission from a REG

In order examine the flicker emission and propagation associated with a REG in the presence of loads distributed along a feeder, consider the radial feeder discussed in Section 2. A distribution system load with a capacity of $P_L + jQ_L$ ($P_L < P_g$ and $Q_L < Q_g$, where P_g and Q_g are generator active power and reactive power output respectively) is connected to the intermediate terminal i in Fig. 1. If the operating power factor angle of the REG and

load are ϕ_g and ϕ_L respectively, the steady-state voltage at the PCC can be written as Eq. (20),

$$\begin{aligned} V_g \approx & V_s + I_g \cdot (R_g \cdot \cos\phi_g + X_g \cdot \sin\phi_g) \\ & - I_L \cdot (R_i \cdot \cos\phi_L + X_i \cdot \sin\phi_L) \end{aligned} \tag{20}$$

where I_L and I_g are steady-state load and generator currents. V_g and V_s are assumed to be in phase. Assuming that the operating power factor of the generator and load do not change, voltage fluctuation at the PCC of the REG due to fluctuation of active power ΔP and reactive power ΔQ of the REG can be given by Eq. (21),

$$\begin{aligned} \Delta V_g \approx & \Delta I_g \cdot (R_g \cdot \cos\phi_g + X_g \cdot \sin\phi_g) \\ & - \Delta I_L \cdot (R_i \cdot \cos\phi_L + X_i \cdot \sin\phi_L) \end{aligned} \tag{21}$$

where ΔI_L, ΔI_g are fluctuations of load current and generator current respectively. If the distribution system load is of constant current type, $\Delta I_L \approx 0$. Hence, the relative voltage fluctuation can be further simplified taking ΔP and ΔQ into account as Eq. (22),

$$\left| \frac{\Delta V_g}{V_g} \right| \approx \left| \frac{R_g \cdot \Delta P + X_g \cdot \Delta Q}{V_g^2} \right| \tag{22}$$

However, according to Eq. (20) the steady-state generator voltage will be less compared to the case where no distribution system loads are connected. Thus, the relative voltage fluctuation at the PCC of the REG in Eq. (22) would be higher compared to that of Eq. (2), leading to increased flicker emission when constant current loads are connected to the feeder. If the distribution system load is of the constant power type, ΔI_L will not be zero as $|\Delta V_i| \geq 0$. Therefore, according to Eq. (A.7) and Eq. (21) ΔV_g will be significant compared to the case of the constant current load; hence, flicker emission will exacerbate further when a constant power load is connected to i^{th} terminal. If the distribution system load is of constant impedance type, flicker emission will be less in comparison to a constant current load (according to Eq. (21) and Eq. (17)), but will be higher compared to the case where there is no load connected to terminal i. Following a similar argument, the flicker level at the i^{th} terminal can be shown to increase when a load is connected to terminal i.

In voltage controlled operation of the REG, the reactive power output of the REG required to maintain the PCC voltage at the reference value will vary when local distribution system loads are connected to the feeder. Therefore, the flicker emission of the REG will be impacted. However, due to the closed loop control in voltage controlled operation, a general conclusion regarding the impact of distribution load on flicker emission cannot be made.

5. Impact of Distribution Loads on Flicker Emission and Propagation in a Wind Farm

In order to demonstrate the impact of distribution system loads on flicker emission and propagation in a distribution network with REG, the MV network discussed in Section 3 was modified by connecting five 11 kV distribution system loads to intermediate terminals T_T1 to T_T5 using five 33/11 kV transformers. The HV network short-circuit capacity and the distribution line impedance was selected as 500 MVA and $0.3 + \mathrm{j}0.3\ \Omega$/km respectively.

Initially, the wind farm was set to operate with a leading power factor of 0.95 in order to maintain the voltage along the feeder within acceptable levels [25]. Flicker levels at each busbar were obtained with various load types connected to intermediate terminals of Fig. 3. The following five scenarios were considered; (a) with no distribution system loads connected to the feeder, (b) constant power loads, (c) constant current loads, (d) constant impedance loads, (e) ZIP loads ($K_1 = K_2 = K_3 = 33.33\%$), each with a capacity of 3.3 MW at 0.9 lagging power factor (f) induction motors with 3.3 MW at 0.9 lagging power factor. Both active and reactive power demand of the loads are greater than the wind power generation, hence, there will be active and reactive power flow from the HV grid. A similar study was conducted, when the wind farm was operating in voltage control mode with a reference voltage of 1.0 p.u.

Fig. 9(a) illustrates that the flicker emission from the wind farm has exacerbated under power factor control operation when the distribution loads are connected to the network for reasons explained in Section 4. Furthermore, the flicker levels at intermediate terminals have also increased. For instance, the flicker levels at all terminals show a 30-40 % increase when constant power loads are connected to the distribution network. The highest flicker levels can be observed in the presence of constant power loads in the network followed by the induction motor loads, constant current loads and constant

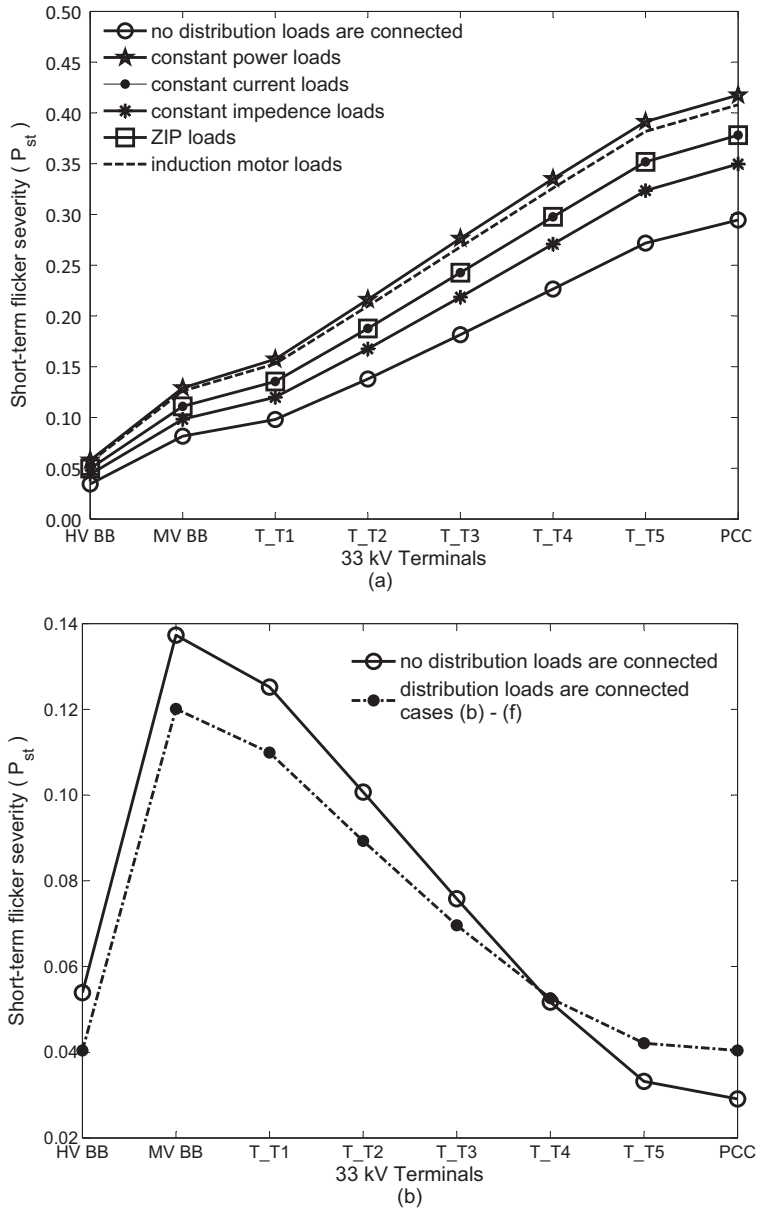

Figure 9: (a) Short-term flicker severity at different terminals when the wind farm operating at a leading 0.95 power factor for cases (a) - (f); (b) Short-term flicker severity at different terminals when the wind farm operating at voltage control mode for cases (a) - (f);

impedance loads. When ZIP loads are connected to the feeder, flicker levels are observed to be equal to that of a constant current load as $K_1 = K_3$, reconfirming the conclusions in Section IV-A (4). Furthermore, in contrary to the common understanding that induction motors aid to attenuate flicker, flicker levels are seen to increase when induction motors are connected. This is due to the fact that voltage variations induced by the wind farm are of low modulation frequencies (generally less than 0.5 Hz), in which flicker is not attenuated by induction motors.

The flicker level for cases (a)-(f), when the wind farm is operating in voltage control mode is given in Fig. 9(b). Flicker emission from the wind farm has slightly increased when the distribution system loads are connected to the feeder due to the increased reactive power requirement (hence, increased reactive power fluctuation) to maintain the PCC voltage, compared to that of case (a). However, there is no distinguishable difference in flicker levels for cases (b)-(f). This is because, the voltage fluctuations arise at the PCC and other terminals do not appreciably differ for cases (b)-(f).

In contrary to the power factor operation, the flicker levels at upstream terminals MV busbar, T_T1, T_T2, have slightly reduced when distribution system loads are connected in voltage control operation. In both operation modes, there is a flow of the active and reactive power from the HV grid to the distribution network to cater for the deficiency between the load demand and wind power generation. Hence, the steady-state voltage at the upstream terminals (i.e. MV busbar, T_T1, T_T2) will be slightly higher compared to the case (a). In power factor control operation the voltage fluctuations due to power fluctuations will increase when distribution loads are connected as explained in Section 4.2. Therefore, the relative voltage fluctuations; hence, flicker will increase when distribution loads are connected compared to that of case (a), irrespective of the increased steady-state voltages in upstream terminals. However, in voltage control operation the relative voltage fluctuations would reduce, leading to less flicker in MV busbar to terminal T_T3, compared to that of case (a).

6. Conclusions

This paper presented a detailed analysis on the impacts of reactive power control strategy of a REG and distribution system loads, in relation to flicker emission and propagation. The study developed mathematical models to exemplify the flicker emission and propagation which were verified through

simulations. The flicker emission from REG, under power factor control operation would exacerbate when operating at both leading and lagging power factors depending on the grid impedance angle. The flicker propagation when a REG is operating at power factor control mode is also dependent on the operating power factor, and grid impedance angle at the point of interest. Furthermore, when the REG is operating in voltage control mode, flicker observed at the PCC of the wind farm would be minimum, however, the flicker levels at upstream of the network would exacerbate. In the power factor control mode, the connection of distribution loads to the local feeder can influence flicker emission from the REG. However, in voltage control mode, the impact of the distribution loads is largely negated by the closed loop controller of the REG. Although, the current research is mainly focused on wind energy generation, the general conclusions would be applicable to any fluctuating generating source connected to distribution feeders.

In the future, distributed generating sources are required to provide increased ancillary services to the network. Therefore, existing flicker standards may need to be augmented to facilitate these services from distributed generators. The work presented in this paper makes contributions towards to the subject of integration of intermittent energy sources to the grid.

Appendix A. Derivation of relative voltage fluctuation transfer coefficient for a constant power load

Assume that a constant power load with a MVA capacity of P_L+jQ_L (load orientation) is connected to a fluctuating voltage source via a line having an impedance of $R_S + jX_S$. The steady-state source voltage phasor ($\mathbf{V_S}$) and load voltage phasor ($\mathbf{V_L}$) can be given by Eq. (A.1),

$$\mathbf{V_S} = \mathbf{V_L} + (R_S + jX_S)\mathbf{I_L} \tag{A.1}$$

$$\mathbf{I_L} = (P_L - jQ_L)/\mathbf{V_L^*} \tag{A.2}$$

Now assume that $\mathbf{V_S}$ fluctuates by $\mathbf{\Delta V_S}$. Accordingly, the load voltage fluctuates by $\Delta\mathbf{V_L}$. Therefore,

$$\mathbf{V_S} + \mathbf{\Delta V_S} = \mathbf{V_L} + \mathbf{\Delta V_L} + (R_S + jX_S)\mathbf{I'_L} \tag{A.3}$$

$$\mathbf{I'_L} = (P_L - jQ_L)/(\mathbf{V_L} + \mathbf{\Delta V_L})^* \tag{A.4}$$

Take $\mathbf{V_L^*}$ as the reference, therefore, $\mathbf{V_L^*} = \mathbf{V_L} = V_L$. Assuming that $\mathbf{V_L}$, $\mathbf{V_S}$, $\Delta\mathbf{V_S}$ and $\Delta\mathbf{V_L}$ are in phase, $\Delta\mathbf{V_S}$ can be written as Eq. (A.5),

$$\Delta V_S = \Delta V_L + Re((R_S + jX_S)\mathbf{\Delta I_L}) \tag{A.5}$$

where $\mathbf{\Delta I_L}$ can be written as Eq. (A.6),

$$\mathbf{\Delta I_L} = \mathbf{I_L} - \mathbf{I'_L} = \frac{P_L - jQ_L}{V_L} - \frac{P_L - jQ_L}{V_L + \Delta V_L} \tag{A.6}$$

Since $V_L \gg \Delta V_L$, $(V_L^2 + V_L \cdot \Delta V_L) \approx V_L^2$. Hence,

$$\mathbf{\Delta I_L} = (P_L - jQ_L)(\frac{-\Delta V_L}{V_L^2}) \tag{A.7}$$

Substitute Eq. (A.7) in Eq. (A.5). Since ΔV_S and ΔV_L are in phase,

$$\left|\frac{\Delta V_L}{\Delta V_S}\right| = \left|\frac{1}{1 - \frac{P_L \cdot R_S + Q_L \cdot X_S}{V_L^2}}\right| \tag{A.8}$$

Furthermore, substitute Eq. (A.2) in Eq. (A.1) and rearrange Eq. (A.1),

$$\left|\frac{V_S}{V_L}\right| = \left|1 + \frac{P_L \cdot R_S + Q_L \cdot X_S}{V_L^2}\right| \tag{A.9}$$

Therefore, the relative voltage fluctuation coefficient can be written as Eq. (A.10),

$$T_{\Delta \mathrm{V_{S,L}}} = \frac{\left|\frac{\Delta V_L}{V_L}\right|}{\left|\frac{\Delta V_S}{V_S}\right|} = \left|\frac{1 + \frac{P_L \cdot R_S + Q_L \cdot X_S}{V_L^2}}{1 - \frac{P_L \cdot R_S + Q_L \cdot X_S}{V_L^2}}\right| \tag{A.10}$$

Appendix B. Network and machine parameters

The network parameters of the HV/MV distribution network in Section 3 and Section 5.
Line parameters:

- impedance of the distribution line 0.4242 Ω/km
- length of the distribution line 15 km

Transformer parameters:

- 132/33 kV transformer: 31.5 MVA, 50 Hz, 0.0034+j0.1020 pu impedance
- 132/33 kV transformer: 5 MVA, 50 Hz, 0.0048+j0.0698 pu impedance

Induction motor parameters:

- 11 kV, 50 Hz, 3.3 MW, efficiency: 96.2%, rated speed: 1485 rpm, no. pole pairs: 2, torque at stalling point : 2.68041 p.u. , inertia: 227.8598 kg.m^2

Doubly-Fed Induction Generator:

- 1.5 MW, rated stator voltage: 0.69 kV, rated rotor voltage: 1863 V, rated apparent power: 1667 kW; rated speed: 1800 rpm; no. pole pairs: 2; stator resistance: 0.01 pu; stator reactance: 0.1 pu; rotor reactance: 0.1 pu; rotor resistance: 0.01 pu; magnetizing reactance: 3.5pu; generator inertia: 75 kg.m^2 turbine inertia: 4,052,442 kg.m^2, shaft stiffness: 83,000,000 Nm/rad

[1] B. Fox, D. Flynn, L Bryans, N. Jenkins, D. Milborrow, M. O'Malley, R. Watson, O. Anaya-Lara, Wind power integration: connection and system operational aspects, First Ed., IET Power and Engineering Series 50, (2007).

[2] M.P. Papadopoulos, S.A. Papathanassiou, S.T. Tentzerakis, N.G. Boulaxis, Investigation of the flicker emission by grid connected wind turbines, Proc. 8th Int. Conf. Harmonics and Quality of Power, Athens, Greece, 1998, pp .1152-1157.

[3] A. Larsson, Flicker emission of wind turbines during continuous operation, Power Engineering Review, IEEE, 2002, pp.59.

[4] M. Machmoum, A. Hatoum, T. Bouaouiche, Flicker mitigation in a doubly fed induction generator wind turbine system, Mathematics and Computers in Simulation, 2010, pp. 433-445.

[5] T Sun, Z. Chen, F. Blaabjerg, Flicker study on variable speed wind turbines with doubly fed induction generators,IEEE Trans. Energy Convers., 2005, pp. 896- 905.

[6] B. Chen, X. Yuan, Y. Xu, X. Wei, Q. Li, R. Sun, J. Song, J. Zhao, Power quality measurement and comparison between two wind farms equipped with FSIG+PMSG and DFIG, Proc. Int. Conf. on Power System Technology, 2010, pp.1-7.

[7] G. Chicco, P. Di Leo, I.-S. Ilie, F. Spertino, Operational characteristics of a 27-MW wind farm from experimental data, Proc. 14th IEEE Mediterranean Electrotechnical Conf., 2008, pp.520-526.

[8] G. Chicco, P. Di Leo, P. Scapino, F. Spertino, Experimental Analysis of Wind Farms connected to the High Voltage Grid: the Viewpoint of Power Quality, Proc. 1st Int. Symp. on Environment Identities and Mediterranean Area, 2006, pp.184-189.

[9] L.S. Christensen, P.E. Sørensen, T.S. Sørensen, H.K. Nielsen, Evaluation of measuring methods for flicker emission from modern wind turbine, AEE TECHWINDGRID09-Grid Integration Seminar, Madrid, Spain, 2009. [online]. Available: http://www.aeeolica.org.

[10] L. Meegahapola, S. Perera, Impact of wind generator control strategies on flicker emission in distribution networks, 15th Int. Conf. Harmonics and Quality of Power, Hong-Kong, 2012.

[11] R. Piwko, P. Meibom,H. Holttinen, S Baozhuang, N. Miller, C. Yongning, W. Weisheng, Penetrating insights: lessons learned from large-scale wind power integration, IEEE Power and Energy Magazine, 2012, pp.44-52.

[12] Y.S. Kim, D. Won, Mitigation of the Flicker Level of a DFIG Using Power Factor Angle Control, IEEE Trans. Power Del, 2008, pp.2457-2458.

[13] M.C. Simoes, S.M. Deckmann, Flicker propagation and attenuation, Proc. 10th Int. Conf. Harmonics and Quality of Power, 2002, pp. 644-648.

[14] E. De Jaeger, G. Borloo, W. Vanceotsem, Flicker transfer coefficient from HV to MV and LV systems, Proc. 14th Int. Conf. Electricity Distribution, (CIRED97), Birmingham, U.K., 1987, pp101-102.

[15] S. Perera, D. Robinson, S. Elphick, D. Geddey, N. Browne, V. Smith, V. Gosbell, Synchronized flicker measurement for flicker transfer evaluation in power systems, IEEE Trans. Power Del, 2006, pp.1477-1482.

[16] Review of flicker Objectives for LV, MV and HV power systems , CIGRE C4.108 Technical Brochure, 2011, ISBN 978-2-85873-138-1.

[17] S . Tennakoon, S. Perera, D. Robinson, Flicker attenuation part I: response of three-phase induction motors to regular voltage fluctuations,IEEE Trans. Power Del, 2008, pp.1207-1214.

[18] S . Tennakoon, S. Perera, D. Robinson, Flicker attenuation part II: transfer coefficients for regular voltage fluctuations in radial power systems with induction motor loads, IEEE Trans. Power Del, 2008, pp.1215-1221.

[19] A.D. Hansen, F. Iov, P.E. Sørensen, N.A. Cutululis, C. Jauch, F. Blaabjerg, Dynamic wind turbine models in power system simulation tool DIgSILENT, Risø report Risø-R-1400(EN), Denmark, 2007.

[20] L. Meegahapola, T. Littler, B. Fox, J. Kennedy, D. Flynn, Voltage and power quality improvement strategy for a DFIG wind farm during variable wind conditions, Proc. Int. Symp. of Modern Electric Power Systems (MEPS), 2010. pp.1-6.

[21] L. Meegahapola, B. Fox, D. Flynn, Flicker mitigation strategy for DFIGs during variable wind conditions," Proc. IEEE PES GM 2010, pp.1-8, 25-29 Jul. 2010.

[22] Technical Rules for the Assessment of Network Disturbances, 2nd Edition, 2007.

[23] A. Kusiak, A. Verma, and X. Wei, Wind Turbine Frontier from SCADA, Wind Systems Magazine, Vol. 3, No. 9, September 2012, pp. 36-39.

[24] DIgSILENT GmbH, DIgSILENT PowerFactory Version 14.1 User's Manual Volume II, May 2011.

[25] Standard Voltages, AS 60038, Standards Australia, 2000.